Available online at www.sciencedirect.com
ScienceDirect
Journal of Nutritional Biochemistry 20 (2009) 45–61
Journal of Nutritional Biochemistry

Phospholipidosis and down-regulation of the PI3-K/PDK-1/Akt signalling pathway are vitamin E inhibitable events associated with 7-ketocholesterol-induced apoptosis

Anne Vejux[a], Stéphane Guyot[c], Thomas Montange[a,b], Jean-Marc Riedinger[d], Edmond Kahn[e], Gérard Lizard[a,b,*]

[a]*Inserm U866, Faculté des Sciences Gabriel, 6 Bd Gabriel, 21000 Dijon, France*
[b]*Université de Bourgogne, Faculté des Sciences Gabriel, Centre de Recherche Inserm –Equipe Biochimie Métabolique et Nutritionnelle, 21000 Dijon, France*
[c]*Laboratoire de Génie des Procédés Microbiologiques et Alimentaires ENSBANA, 1 Esplanade Erasme, 21000 Dijon, France*
[d]*Centre Anti-Cancer GF Leclerc, Laboratoire de Biologie Médicale, 21000 Dijon, France*
[e]*INSERM UMR S 678 UPMC, CHU Pitié-Salpêtrière, 75634 Paris Cedex 13, France*

Received 26 October 2007; received in revised form 6 December 2007; accepted 7 December 2007

Abstract

Among the oxysterols accumulating in atherosclerotic plaque, 7-ketocholesterol (7KC) is a potent apoptotic inducer, which favours myelin figure formation and polar lipid accumulation. This investigation performed on U937 cells consisted in characterizing the myelin figure formation process; determining the effects of 7KC on the PI3-K/PDK-1/Akt signalling pathway; evaluating the activities of vitamin E (Vit-E) (α-tocopherol) on the formation of myelin figures and the PI3-K/PDK-1/Akt signalling pathway and assessing the effects of PI3-K inhibitors (LY-294002, 3-methyladenine) on the activity of Vit-E on cell death and polar lipid accumulation. The ultrastructural and biochemical characteristics of myelin figures (multilamellar cytoplasmic inclusions rich in phospholipids and 7KC present in acidic vesicles and the reversibility of these alterations) support the hypothesis that 7KC is an inducer of phospholipidosis. This oxysterol also induces important changes in lipid content and/or organization of the cytoplasmic membrane demonstrated with merocyanine 540 and fluorescence anisotropy, a loss of PI3-K activity and dephosphorylation of PDK-1 and Akt. It is noteworthy that Vit-E was able to counteract phospholipidosis and certain apoptotic associated events (caspase activation, lysosomal degradation) to restore PI3-K activity and to prevent PDK-1 and Akt dephosphorylation. When Vit-E was associated with LY-294002 or 3-methyladenine, impairment of 7KC-induced apoptosis was inhibited, and accumulation of polar lipids was less counteracted. Thus, 7KC-induced apoptosis is a PI3-K-dependent event, and Vit-E up- and down-regulates PI3-K activity and phospholipidosis, respectively.

Keywords: Akt; PI3-K; 7-ketocholesterol; Phospholipidosis; Vitamin E

1. Introduction

Oxysterols are 27 carbon derivatives of cholesterol containing additional oxygen atoms on the steroid's nucleus or on the side chain [1]. They are common components of oxidized lipoproteins (Ox-LDL), which play key roles at different stages of the atherosclerotic process [2] and comprise a large family of molecules resulting either from the auto-oxidation of cholesterol in air or from the enzyme-catalyzed transformation of cholesterol in various cell species [3]. Until now, the role played by oxysterols in the development of atherosclerotic lesions has been widely suspected for the following reasons: numerous studies

Abbreviations: AO, acridine orange; DMSO, dimethylsulfoxide; DPH, 1,6-diphenyl-1,3,5-hexatriene; FLICA, fluorochrome-labelled inhibitor of caspases; 7KC, 7-Ketocholesterol; MC540, merocyanine 540; 3MA, 3-methyladenine; MDC, monodansylcadaverine; NR, Nile Red; PDK-1, 3′Phosphoinositide-regulated kinase-1; PI3-K, phosphoinositide 3-kinase; PBS, phosphate-buffered saline; PI, propidium iodide; PP2A, protein phosphatase 2A; TMSE, Trimethylsilylethanol; TPBS, 0.1% Tween 20, phosphate buffered saline; Vit-E, vitamin E.

* Corresponding author. Tel.: +33 380 39 62 56; fax: +33 380 39 62 50.
E-mail address: gerard.lizard@u-bourgogne.fr (G. Lizard).

0955-2863/$ – see front matter © 2009 Elsevier Inc. All rights reserved.
doi:10.1016/j.jnutbio.2007.12.001

determined increased oxysterol levels in the plasma of atherosclerotic patients and in atheromatous plaque [mainly 27-hydroxycholesterol, 7-ketocholesterol (7KC) and 7β-hydroxycholesterol] [4], and several investigations clearly established that some of these compounds (7β-hydroperoxycholesterol, 7β-hydroxycholesterol and 7KC) mimic the cytotoxic effects of Ox-LDL on the cells of the vascular wall [2]. Moreover, some oxysterols, especially 7KC and 7β-hydroxycholesterol, which are also present at important levels in some processed foods, have potent cytotoxic, pro-oxidative and/or proinflammatory properties [5,6], which are hallmarks of the pathophysiological mechanisms involved in the atherosclerotic process [2,3,7].

Of the different oxysterols capable of promoting atherogenesis, 7KC is one of the most abundant in plasma and arterial lesions of atherosclerotic patients [3]. It has been clearly established, particularly on human promonocytic U937 cells, that this oxysterol induces a complex mode of cell death with some characteristics of apoptosis: externalization of phosphatidylserine; loss of transmembrane mitochondrial potential ($\Delta\Psi$); mitochondrial release of cytochrome *c*; endonuclease G and apoptosis-inducing factor; cleavage of Bid; activation of caspases 2, 3, 7, 8 and 9; degradation of poly(ADP-ribose)polymerase and inhibitor caspase-activated deoxyribonuclease, internucleosomal DNA degradation and condensation/fragmentation or swelling of the nuclei, which are associated with the formation of multilamellar cytoplasmic structures [5,6,8]. These multilamellar cytoplasmic structures, isolated by subcellular fractionation after staining with monodansylcadaverine (MDC), have been partially characterized: they accumulate 7KC and also contain high amounts of phosphatidylcholine and sphingomyelin [9]. It is noteworthy that ultrastructurally similar MDC-positive multilamellar bodies, considered autophagic vacuoles, were observed in Mv1Lu mink lung type II alveolar cells transfected with β1-6-*N*-acetylglucosaminyl transferase V [10]. Based on ultrastructural and biochemical criteria, it was assumed that 7KC-induced cell death might also be associated with an autophagic process [11,12]. Moreover, since a close relation may exist between autophagy and apoptosis [13], and since the phosphoinositide 3-kinase (PI3-K)/Akt pathway is an important second messenger system involved in both autophagy [14] and apoptosis [15], it was important to determine the role played by the PI3-K/Akt signalling pathway in 7KC-induced cell death. Akt, which was initially identified as the mammalian homologue of the viral oncogene v-akt, is also called "protein kinase B" (PKB) [16]. A probable inactivation of the PI3-K/Akt signalling pathway in 7KC-induced cell death was suggested by a previous investigation demonstrating an activation of the proapoptotic protein BAD (Bcl-xl/Bcl-2 associated death promotor), which is present in its dephosphorylated form in 7KC-treated cells [17]. Indeed, when Akt is activated and presents in its phosphorylated form, via the PI3-K kinase signalling pathway through the 3-phosphoinositide-dependent protein kinase-1 (PDK-1), it maintains BAD in its inactive form by phosphorylation on serine 99 [15].

Based on these different considerations, the aim of the present study conducted on untreated and 7KC-treated human promonocytic U937 cells and, in part, on rat A7R5 aortic smooth muscle cells, was: (1) to characterize the cellular process associated with the formation of multilamellar structures (also called myelin figures) observed with 7KC treatment as well as with other cytotoxic oxysterol treatments [5,8,11] and to rely the formation of these myelin figures with cell death; (2) to determine the effects of 7KC on the PI3-K/PDK-1/Akt signalling pathway; (3) to evaluate the effects of vitamin E (Vit-E; α-tocopherol) on the formation of myelin figures and on the PI3-K/PDK-1/Akt signalling pathway, since we previously described an impairment of 7KC-induced apoptosis by Vit-E [18]; and (4) to determine the effects on various PI3-K inhibitors (LY-294002, 3-methyladenine) on the activity of Vit-E. The role played by the protein kinase PI3-K was investigated since Akt/PKB regulates B-cell lymphoma (BCL) family members during oxysterol-induced apoptosis [19].

We report that 7KC-induced myelin figures are acidic phospholipid-rich vesicles, also accumulating 7KC and cholesterol. Thus, it was demonstrated that 7KC is a potent inducer of phospholipidosis [20,21], which precedes early signs of cell death such as the loss of transmembrane mitochondrial potential and morphological nuclear changes. In addition, we show that 7KC-induced cell death and phospholipidosis are counteracted by Vit-E, which is also capable of restoring the loss of PI3-K activity and the dephosphorylation of PDK-1 and Akt triggered by 7KC. However, the impairment of 7KC-induced apoptosis by Vit-E was inhibited by LY-294002 and 3-methyladenine, and the decrease in polar lipid accumulation was almost abolished when Vit-E was associated with LY-294002 and 3-methyladenine.

2. Materials and methods

2.1. Cells and treatments

Human promonocytic leukaemia cells (U937) obtained from the American Type Culture Collection (Manassas, VA, USA) were used. U937 cells were grown in RPMI 1640 with GlutaMAX I (Gibco, Eragny, France) and antibiotics (Invitrogen, Cergy-Pontoise, France) supplemented with 10% (v/v) heat-inactivated fetal calf serum (Gibco); they were seeded at 500,000/ml culture medium and passaged twice a week.

The 7KC was provided by Sigma (L'Isle d'Abeau Chesnes, France), and its purity was determined to be 100% by gaseous phase chromatography coupled with mass spectrometry. For all experiments, a stock solution of 7KC was prepared at a concentration of 800 μg/ml, as previously described [5]. In all experiments conducted on U937 cells, 7KC was added to the culture medium containing 10% heat-

inactivated fetal calf serum (or 10% heat-inactivated delipidized or delipoproteinized serum) (Sigma) at the beginning of the culture at final concentration of 20 μg/ml (50 μM) or 40 μg/ml (100 μM), and treatments were carried out for 6, 14, 18, 24 and/or 30 h. When U937 cells were cultured in the presence of 7KC associated with α-tocopherol (Vit-E) or with different inhibitors of autophagy (mixture of amino acids, wortmannin, 3-methyladenine or okadaic acid), as well as with inhibitors of PI3-K (LY-294002, 3-methyladenine) [22], these compounds were always added to the culture medium 30 min before 7KC. When Vit-E was associated with PI3-K inhibitors, these compounds were simultaneously added 30 min before 7KC. Vit-E corresponding to DL-α-tocopherol was provided by Sigma, and its purity was 95%. The Vit-E solution was extemporaneously prepared at 30 mM in ethanol (1 mg of α-tocopherol/50 μl ethanol), and diluted in the culture medium to obtain a 100-μM final concentration. The mixture of amino acids was a generous gift from Dr Codogno (Inserm U756, Chatenay Malabry, France). In this initial mixture, amino acids (prolin, histidine, methionine, tryptophane, leucin, cysteine, glutamic acid, glycine, isoleucine, lysin, serine, threonine, valine, phenylalanine, asparagine, tyrosin, alanine, glutamine, aspartic acid, arginine) were present at 37.5 or 500 mM. This mixture was added to the culture medium to obtain amino acids at 3- and 40-mM final concentrations. A stock solution of wortmannin (Sigma) was prepared at 2.3 mM by dilution in DMSO (Sigma), stored at 4°C and used at 10 nM. The 3-methyladenine (Sigma) was extemporaneously prepared in warm water at 100 mM and used at a 10-mM final concentration. Okadaic acid (Sigma) was prepared at 10 μM in DMSO and used at 7.5 nM. LY-294002 (Sigma) was prepared at 10 mM in DMSO and used at 40 μM.

2.1.1. In situ detection of activated caspases with fluorochrome-labelled inhibitor of caspases

Total caspase activity was measured with fam-VAD-fmk (Trevigen, Gaithersburg, MD, USA) using a specifically dedicated kit according to the manufacturer's suggested procedures. Fluorochrome-labelled inhibitor of caspases (FLICA) reagent (fam-VAD-fmk) is a cell permeant and noncytotoxic compound widely used in flow cytometry and microscopy to investigate caspase activities [23]. FLICA reagent was used as previously described [24].

2.1.2. Staining conditions with Hoechst 33342

Nuclear morphology was analysed after staining with Hoechst 33342 (10 μg/ml), and apoptotic cells were characterized by condensed and/or fragmented nuclei [25]. Cell deposits were observed under ultraviolet light by fluorescence microscopy with an Axioskop right microscope Zeiss, Jena, Germany). For each sample, 300 cells were examined.

2.1.3. Staining conditions with MDC

Myelin figures were stained with MDC (λEx_{max}=340 nm, λEm_{max}=530 nm; Sigma). MDC is a lysosomotropic agent and a solvent polarity probe accumulating in acidic compartments, probably because of its amino group, which becomes protonated at low pH, leading to an ion-trapping mechanism [9,26]. The protocol used was described by Kahn et al. [9].

2.1.4. Staining conditions with Nile red

Nile Red (NR) is a phenoxazine dye used on living cells to localize and quantify neutral and polar lipids (Sigma). NR stains neutral lipids yellow (570–590 nm) and polar lipids orange/red (590 nm and above) when excited at 488 nm [27]. When excited at 532 nm, NR can identify polar lipids, which are colored in orange/red [28]. In the present investigation, NR was prepared at 100 μg/ml in DMSO and used as previously described [28].

2.2. Staining conditions with merocyanine 540

Merocyanine 540 (MC540) (Sigma) is a negatively charged chromophore that binds to the outer leaflet of the cell membrane [29]. The loss of asymmetry and altered packing of the membrane enhance MC540 fluorescence [29]. MC540 was prepared in absolute ethanol (2 mg/ml) and added to the culture medium at 2.5 μg/ml. After 10 min of incubation at room temperature, cells were analysed by flow cytometry. MC 540 bright cells and MC 540 dim cells were considered as apoptotic and normal cells, respectively [30]. Flow cytometric analyses were performed on a Cyflow Green flow cytometer (Partec, Münster, Germany) equipped with a green laser (Nd:YAG) emitting at 532 nm and working at 50 mW. The fluorescence of MC540 was collected through a 590/30-nm band pass filter and measured on a logarithmic scale. A total of 10,000 cells were acquired for each sample, and data were analysed with the FlowMax software (Partec). Data were expressed by the [MC 540 bright cells]/[MC 540 dim cells] ratio.

2.2.1. Staining conditions with oil red o and the Ziehl–Neelsen procedure

The presence of neutral lipids was also investigated with Oil Red O (Sigma). This stain is soluble in neutral lipids and remains dissolved in triglycerides after washing. To this end, cells were applied to glass slides by cytocentrifugation (5 min, 1,000 rpm) with a cytospin 4 (Shandon, Cheshire, UK). Cell deposits were then washed with distilled water and incubated in isopropanol (60%) for 1 min. Cells were further stained with Oil Red O for 15 min and incubated for 1 min in isopropanol (60%). After washing in distilled water, nuclei were stained with hemalum (2–3 min). After washing in water, the preparation was mounted in Eukitt and stored in the dark at room temperature until observations with an Axioskop right microscope (Zeiss).

Ziehl Neelsen staining is an acid-fast stain test, which is used to evaluate the presence of ceroids [31]. These lamellar structures belong to the lipofuscin group of pigments and originate from oxidation and peroxidation of phospholipids and unsaturated fatty acids [32]. Staining was done by applying cells to glass slides by cytocentrifugation (5 min,

1,000 rpm) with a cytospin 4 (Shandon), fixed and stained with fuchsin for 15 min. After washing with water, cell preparations were incubated in Gabett solution (methylene blue, sulfuric acid 60°, absolute alcohol, distilled water) for 5 min. After washing, cell preparations were air-dried, mounted in Dako Mounting medium (Dako, Copenhagen, Denmark) and stored in the dark at room temperature until observations with an Axioskop right microscope (Zeiss).

2.2.2. Staining conditions with acridine orange

Lysosomal destabilization was assayed by staining with acridine orange (AO) (Sigma). AO is a lysosomotropic weak base, which produces a red fluorescence when excited by a blue light [33]. During prolonged exposure to cytotoxic agents, the red fluorescence of AO decreases markedly [34]. The shift in AO fluorescence from granular red to diffuse green reflects leakage and redistribution of AO from the lysosomes, indicating impairment of the lysosome membranes or the inability of the lysosomes to maintain low pH. The method used has been previously described [5].

2.2.3. Detection of LC3 II by indirect immunofluorescence

U937 cells cultured in the absence or presence of 7KC (20 μg/ml) were applied to glass slides by cytocentrifugation (5 min, 1,000 rpm) with a cytospin 4 (Shandon). Glass slides were treated at room temperature with 2% formol and then washed with phosphate-buffered saline (PBS). The cells were further incubated (45 min, 37°C) with a rabbit polyclonal LC3 II antibody (a generous gift from Dr T Yoshimori, National Institute of Genetics, Mishima, Japan) diluted 1:10 in PBS containing 1% bovine serum albumin (PBS-1%BSA). After washing (PBS), cells were incubated (30 min, 37°C) with a biotinylated Multilink antibody (Dako) diluted 1:100 in PBS-1%BSA. After washing (PBS), cells were incubated (30 min, 37°C) with streptavidin-Texas Red (Molecular Probes) diluted 1:100 in PBS-1%BSA. After washing (PBS), glass slides were mounted in Fluoprep (Bio-Mérieux, Marcy l'Etoile, France), coverslipped and stored in the dark at 4°C until microscopical examinations. Observations were made with an Axioskop fluorescent microscope (Zeiss).

2.2.4. Transmission electron microscopy

For electron microscopy, $5-10\times10^6$ cells were fixed for 1 h with 2% glutaraldehyde prepared in 0.1 mM cacodylate buffer (pH 7.4), postfixed in osmium tetroxide, dehydrated with graded ethanol series and embedded in Epon. Sections were stained with uranyl acetate and lead citrate and examined with an H600 electron microscope (Hitachi, Tokyo, Japan).

2.2.5. Fluorescence anisotropy

The lipid organization of cytoplasmic membrane was investigated by fluorescence anisotropy [35] on U937 cells cultured for 18 h in the absence or presence of 7KC (40 μg/ml) associated or not with Vit-E (100 μM). The plasma membrane of cells was labelled with the fluorescent probe 1,6-diphenyl-1,3,5-hexatriene (DPH, Sigma). The stock-solution concentration of DPH in tetrahydrofuran (Sigma) was 1 mM and it was stored in the dark at −30°C.

A fluorolog-3 spectrofluorometer with a T configuration was used to measure the fluorescence anisotropy of DPH (HORIBA Jobin Yvon, Longjumeau, France). An ozone-free xenon lamp exhibiting a characteristic peak around 467 nm was used as the light source. Excitation and emission wavelengths were 360 nm (5-nm bandwidth) and 430 nm (5-nm bandwidth), respectively. Samples were added to a 1-cm path-length spectroscopic quartz cuvette (VWR International, Limonest, France). The cuvette was placed in a stirred and thermostat-controlled chamber in the spectrofluorometer. Temperature, maintained at 37°C, was regulated using a Peltier temperature control unit and a K-thermocouple (TCSA, Dardilly, France) was added to the cuvette in order to read the temperature of the cell suspension. Briefly, at the end of the incubation time (18 h), the cells were centrifuged for 5 min at 150 g at 16°C, and the cell pellet was washed twice in a volume of PBS (pH 7.4) composed of phosphate buffer (0.01 M), potassium chloride (0.0027 M) and sodium chloride (0.137 M). Then 3 ml of the cell suspension, adjusted to 1×10^6 cells/ml, were added to the quartz cuvette, and 4 μl of DPH stock solution was added. DPH concentration was 1 μM. Fluorescence anisotropy (r) was measured during a 10-min plateau phase at 37°C.

The r value, which is defined as the linearly polarized component's intensity divided by the total light intensity, was calculated using Equation 1:

$$r = \frac{I_{VV} - GI_{VH}}{I_{VV} + 2GI_{VH}} \quad (1)$$

where I_{VV} and I_{VH} are the measured fluorescence intensities with the excitation polarizer vertically oriented and the emission polarizer both vertically and horizontally oriented. G is the grating correction factor defined by Equation 2:

$$G = \frac{I_{HV}}{I_{HH}} \quad (2)$$

where I_{HV} and I_{HH} are the measured fluorescence intensities with the excitation polarizer horizontally oriented and the emission polarizer vertically and horizontally oriented, respectively.

The signal-to-noise ratio of I_{VV} measurements was in the range of 8–40. Results are given as a mean. All experiments were repeated at least three times using three independent experiments.

2.2.6. Subcellular fractionation and biochemical characterization of monodansylcadaverin and NR-positive cytoplasmic structures

The methodology used to isolate multilamellar cytoplasmic structures (also called myelin figures) by subcellular fractionation was described by Biederbick et al. [26]. After 24 h of culture in the absence or presence of 7KC (20 μg/ml), U937 cells were incubated at 37°C with MDC (0.05 mM, 15 min) or NR (0.1 μg/ml, 15 min). Cells ($150–200\times10^6$) were then

washed with cold PBS, resuspended in a homogenization buffer (10 mM Tris HCl, pH 8, 0.25 M sucrose, 1 mM dithiothreitol, 0.1 mM phenylmethylsulfonyl fluoride, 3 mM $MgSO_4$ and 10 mM NaCl) and centrifuged (700*g*, 10 min, 4°C). The pellet was resuspended in 1 ml Tris HCl (10 mM, pH 8) and separated on a continuous sucrose gradient (10–60%) at 112,500 g for 5 h using a R70.1 rotor in a Beckman Optima L-90K centrifuger. Fractions were collected from the bottom of the gradient. A LS50B Perkin Elmer spectrofluorometer was used to detect MDC ($\lambda_{Excitation}$= 340 nm, $\lambda_{Emission}$=530 nm) and NR-labelled compartments ($\lambda_{Excitation}$=488 nm, $\lambda_{Emission}$=600 nm). The sucrose density of each fraction was simultaneously measured using a Codiam Scientific refractometer. For each fraction, the lipid content of cholesterol (esterified and unesterified), 7KC and phospholipids (phosphatidylcholine, sphingomyelin) was determined.

2.2.7. Characterization and quantification of cholesterol and 7KC using capillary gas chromatography

After various culture times, the cellular suspension was centrifuged and cells and surnageant were separated. Cells were numerated and washed twice with PBS 1X. The lipids were extracted from 1.5–3×10^6 cells using Folch reagent containing 0.05% butylated hydroxytoluene as antioxidant [36]. The lipids were saponified overnight in the dark, in argon and at room temperature using 1 M potassium hydroxide (10 ml). After adding 20 ml purified water, nonsaponifiable matter was extracted twice by 20 ml dichloromethane. The two dichloromethanolic fractions ware gathered and washed several times with water until a neutral pH was reached. We used 5α-cholestane as external standard.

Before analysis, the samples were transformed in trimethylsilylether (TMSE) derivatives as follows: after evaporation of the solvent in nitrogen, the samples were redissolved in 100 μl of pyridine, and 100 μl of *N*,*O*-bis-(trimethylsilyl)trifluoroacetamide containing 1% trimethylchlorosilane (Supelco, Bellefonte, PA, USA) were added. The TMSE derivatives were obtained by heating (30 min, 60°C). The reagents were then evaporated in nitrogen and the residue dissolved in hexane for gas chromatography analysis. The analyses were performed using a 5890 Series II Hewlett Packard gas chromatograph (Palo Alto, CA, USA), equipped with a needle-falling injector (temperature 290°C) and a flame ionization detector operating at 300°C. One column was used: a 0.25-μm film thickness and a 30-m×0.25-mm internal diameter DB5-MS fused silica capillary column (J&W Scientific, Folsom, CA, USA). Helium was the carrier gas. After 1 min at 50°C, the oven temperature was raised from 50 to 275°C at 20°C/min, then 1°C/min to 290°C. The analyses were done at 290°C. The chromatographic data were analyzed using Diamir software (JMBS Developments, Fontaine, France).

2.2.8. Characterization and quantification of phospholipids by quantitative liquid chromatography/mass spectrometry

Lipids were extracted according to the method developed by Folch et al. [36]. Dimyristoylphosphatidylcholine (DMPC, Sigma) and lauroylsphingomyelin (LSM, Sigma) were used as internal standards, and 50 mg/l butylated hydroxytoluene was added to the solvent. An aliquot of the chloroformic phase was evaporated, and 100 μl chloroform/methanol (4/1) was added for quantitative liquid chromatography/mass spectrometry. Phospholipid analysis was performed on a Hypersil Si 2∗200 mm column (Agilent Technologies, Santa Clara, CA, USA) with a binary gradient of solvent A [5 mM ammonium acetate in chloroform/methanol (4/1)] and solvent B [5 mM ammonium acetate in chloroform/methanol/water (6/3.4/6)] [37]. The combination was eluted at a flow rate of 0.3 ml/min. Positive ESI-MS was performed on a MSD 1100 Mass Spectrometer (Agilent Technologies). The orifice voltage was set at 120 V, the capillary voltage at 3.5 kV, the drying gas (nitrogen) flow at 8 l/min and the scan range from m/z 400 to 950. Concentrations were determined from the ratio of the peak area of phosphatidylcholine and sphingomyelin to the peak area corresponding to the internal standard. Integrated peak areas from extracted ion chromatograms (EIC) for *m*/*z*=700–950 at the retention time (RT) of phosphatidyl choline (PC) or sphingomyelin (SM) were divided by the EIC for *m*/*z*=679 at the RT of DMPC or *m*/*z*=647 at the RT of LSM. Levels were determined by comparing this ratio with a standard curve of known amounts of phosphatidylcholine and sphingomyelin.

2.2.9. Protein extraction and western blot analysis

Cells were resuspended in Ripa lysis buffer (0.1% (w/v) sodium dodecyl sulfate (SDS), 1% (w/v) Igepal, 0.5% (w/v) Na-desoxycholate, 50 mM Tris–HCl pH 8, 150 mM NaCl) containing a mixture of protease and phosphatase inhibitors (0.1 mM phenylmethanesulfonyl fluoride, 2.5 μg/l aprotinin, 10 μg/l pepstatin A, 2.5 μg/l trypsin inhibitor, 2.5 μg/l leupeptin, 0.1 mM orthovanadate, 40 mM β-glycerophosphate, 100 mM NaF). After 30 min incubation at 4°C in the lysis buffer, the cell debris were eliminated by centrifugation (20 min, 10,000*g*) and the supernatant was collected.

The protein concentrations were measured using bicinchoninic acid reagent (Pierce, Rockford, IL, USA) according to the method of Smith et al. [38]. Eighty micrograms of protein per slot were diluted in loading buffer [125 mmol/l Tris/HCl, pH 6.8, 10% (w/v) mercaptoethanol, 4.6% (w/v) SDS, 20% (v/v) glycerol, 0.003% (w/v) Bromophenol blue), boiled for 3 min, separated by SDS-polyacrylamide gel electrophoresis (SDS-PAGE) (30% acrylamide stacking gel; 10% acrylamide migration gel) for 30 min at 50 V and 1 h at 80 V using the Mini Protean II (Bio-Rad, Ivry-sur-Seine, France) and electroblotted onto a polyvinylidene difluoride membrane for 45 min at 80 V at 4°C (Bio-Rad). After blocking nonspecific binding sites for 2 h at room temperature in TPBS ($NaCl/P_i$, 0.1% Tween-20), the membranes were incubated overnight at 4°C with various primary antibodies diluted in TPBS. The anti-Akt polyclonal antibody (dilution: 1:1000), the anti-Akt phospho Thr 308 polyclonal antibody (dilution: 1:1000) and the anti-PDK-1 phospho Tyr 373/376 polyclonal antibody (dilution: 1:1000) were purchased

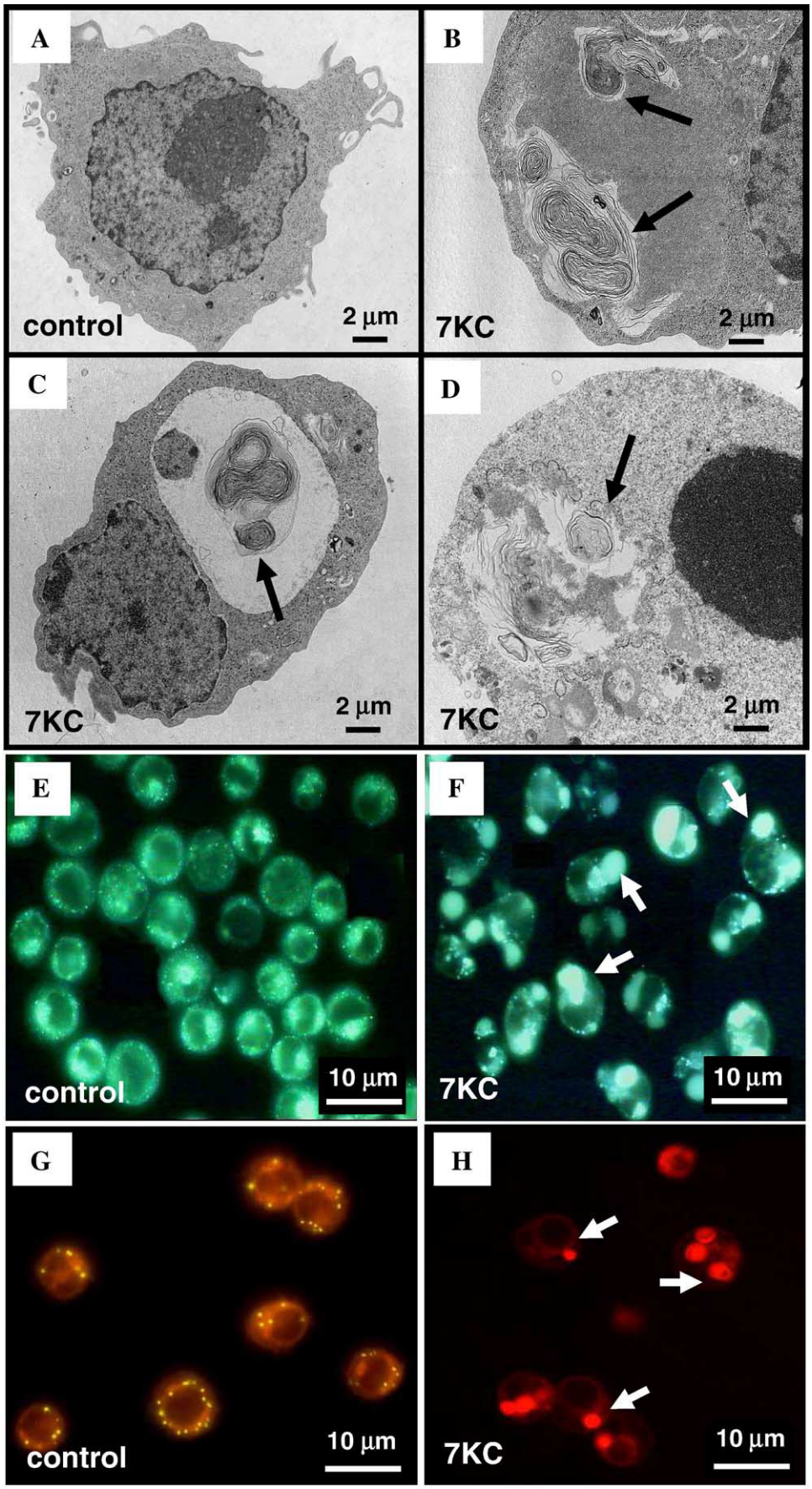
A
control
2 µm
B
7KC
2 µm
C
7KC
2 µm
D
7KC
2 µm
E
control
10 µm
F
7KC
10 µm
G
control
10 µm
H
7KC
10 µm

from Cell Signaling Technology (Danvers, MA, USA). The anti-PDK-1 monoclonal antibody (dilution: 1:100) and the anti-Hsc-70 polyclonal antibody (dilution: 1:1000) were purchased from Santa Cruz Biotechnology (Santa Cruz, CA, USA). After three 10-min washes with TPBS, the membranes were incubated with horseradish peroxidase-conjugated secondary antibody (Dako) at a 1:2500 dilution for 1 h at room temperature and washed three times in TPBS for 10 min. Color protein markers (Cambrex, Charles City, IA, USA) were used to specifically identify the bands of interest, and autoradiographs of the immunoblots were taken using an enhanced chemoluminescence detection kit (Amersham, Les Ulis, France). When the membrane was only incubated with the secondary antibody, no band was observed.

2.2.10. Measurement of PI3-K activity

We determined PI3-K activity by measuring the amount of PI(3,4,5)P_3 extracted from cells by means of a standard enzyme-linked immunosorbent assay format. We used the PIP_3 Mass ELISA kit (Echelon Biosciences, Salt Lake City, UT, USA). PI(3,4,5)P_3 was extracted according to the following protocol. The cells (5×10^6 cells) were collected and centrifuged (525*g*, 5 min, 4°C). The pellet was resuspended in a solution of 5% TCA/1 mM EDTA and centrifuged (525*g*, 5 min). This step was repeated once. Neutral lipids were extracted by adding a solution of MeOH:$CHCl_3$ (2:1), the suspension was vortexed three times over 10 min at room temperature, then centrifuged (525*g*, 5 min). This step was repeated once again. Acidic lipids were extracted by adding a solution of MeOH:$CHCl_3$:12 M HCl (80:40:1), the suspension was vortexed four times over 15 min at room temperature, then centrifuged (525*g*, 5 min). The supernatant was mixed with $CHCl_3$ and HCl (0.1 M), and this suspension was centrifuged (525*g*, 5 min) to separate organic and aqueous phases. The organic phase was collected and dried in a vacuum dryer. Dried lipids were resuspended in PIP_3 buffer (50 mM HEPES, 150 mM NaCl, 1.5% Na Cholate, pH 7.4), sonicated in a water bath for 5 min and left overnight at 4°C. After this extraction, ELISA was used according to the manufacturer's procedure (Echelon Biosciences).

2.2.11. Statistical analysis

Statistical analysis was performed using WinSTAT software (Microsoft, Redmond, WA, USA). The Student *t* test or the Mann–Whitney *U* test were used to compare the different groups, and data were considered statistically different at a *P* value of .05.

3. Results

3.1. Induction of phospholipidosis on 7KC-treated cells

In agreement with our previous investigations [5,9,11], we confirm that 7KC used at 20 or 40 μg/ml for 18, 24 and/or 30 h is a potent inducer of cytoplasmic multilamellar structures (myelin figures) (Fig. 1A–D) and favours substantial accumulation of the lysosomotropic dye MDC (Fig. 1E–F). As this accumulation of MDC was not counteracted by potent inhibitors of autophagy [mixture of amino acids (0.5–3 mM); 3-methyladenine (10 mM); okadaic acid (7.5 nM); wortmannin (10 nM)], the present data rather suggest that these MDC-positive cytoplasmic structures are not autophagic vesicles, whereas LC3-II (often considered as a marker of autophagy) [12] was detected by indirect immunofluorescence staining on 7KC-treated cells (data not shown). In addition, the absence of spontaneous orange-yellow fluorescence emission in 7KC-treated cells examined under UV light and the lack of staining with the Ziehl-Neelsen solution do not support the argument that 7KC-induced myelin figures are ceroid structures which also have a multilamellar aspect in transmission electron microscopy [39]. Moreover, when the cells were stained with NR, which stains neutral and polar lipids yellow and red, respectively [27], a large number of yellow fluorescent spots were revealed in the cytoplasm of untreated cells (Fig. 1G). However, only a few yellow cytoplasmic fluorescent spots were observed in 7KC-treated cells, whereas mainly large orange-red cytoplasmic fluorescent structures were detected (Fig. 1H). Moreover, in agreement with our data obtained with NR, untreated cells were slightly stained with Oil Red O, which identifies neutral lipids, whereas no staining was found on 7KC-treated cells (data not shown). These different cytological characterizations were associated with biochemical studies. Untreated and 7KC-treated cells, stained either with MDC or NR, were fractionated by ultracentrifugation using the procedure described by Biederbick et al. [26] to isolate multilamellar cytoplasmic structures. The cellular fractions corresponding to a sucrose density from 22% to 28% were strongly stained with MDC and NR (Table 1). Therefore, these fractions were pooled and characterized by gas chromatography coupled with mass spectrometry. It is worth noting that MDC- and NR-positive fractions have similar lipid profiles: they contain high levels of cholesterol and phospholipids (phosphatidylcholine, sphingomyelin) and accumulate 7KC (Table 1). Interestingly, when 7KC-treated cells were cultured in the

Fig. 1. Ultrastructural and cytological characterization of 7KC-induced phospholipidosis. Identification of multilamellar cytoplasmic structures (myelin figures) using transmission electron microscopy. Transmission electron microscopy of U937 cells cultured in the absence (A) or presence (B–D) of 7KC (20 μg/ml; 50 μM) for 30 h. Myelin figures (arrows) were only observed in 7KC-treated cells. They can have various sizes and shapes. Staining with MDC, a solvent polarity probe accumulating in acidic compartments. Observations using fluorescence microscopy of U937 cells cultured in the absence (E) or presence (F) of 7KC (40 μg/ml; 100 μM) for 24 h. Cellular structures stained by MDC are indicated by arrows. Staining with NR, emitting a yellow or orange-red fluorescence in the presence of neutral or polar lipids (including phospholipids), respectively, when excited by a blue light. After 24 h of culture, various numbers of punctuated yellow cytoplasmic spots are observed in untreated U937 cells (G), whereas large orange-red cytoplasmic structures, indicated by arrows, are mainly present in the cells treated with 7KC (40 μg/ml) (H).

presence of 7KC for periods of time preceding the loss of transmembrane mitochondrial potential, considered a point of non-return [40] and re-introduced in 7KC-free medium, the percentage of cells with depolarized mitochondria was sharply reduced, and lower levels of polar lipids per cell (evaluated by staining with NR and characterized by large red cytoplasmic structures) were found (Fig. 2). Thus, our data demonstrate that 7KC-induced myelin figure formation is associated with the following cellular events: (1) accumulation of polar lipids, as shown by NR staining and biochemical analysis (high levels of phospholipids, mainly phosphatidylcholine and sphingomyelin in myelin figures isolated after staining with MDC or NR); (2) location of myelin figures in acidic compartments (staining with MDC); 3) accumulation of 7KC in myelin figures and (4) reversibility of polar lipid accumulation. Taken together, these different observations lead us to conclude that 7KC is a potent inducer of phospholipidosis with the following criteria: excessive accumulation of phospholipids in cells; ultrastructural appearance of multilamellar cytoplasmic inclusions, predominantly lysosomal in origin; accumulation of the inducing drug in association with phospholipids in multilamellar structures; and reversibility of alterations after discontinuance of drug treatment [20,21].

In addition, when U937 cells and rat smooth muscle cells (A7R5) were cultured in the presence of 7KC in culture medium containing 10% fetal calf serum, 10% delipoproteinized fetal calf serum or 10% delipidized serum, we observed similar cytotoxic effects (increased permeability to propidium iodide, simultaneous presence of cells with swollen, condensed and fragmented nuclei) and a comparable accumulation of polar lipids revealed by staining with NR (our data not shown). Therefore, these observations lead us to conclude that the accumulation of polar lipids does not require extracellular lipids and is the consequence of an altered cellular lipid metabolism triggered by 7KC. Taken together, these data bring additional evidences on the potential roles of oxysterols to favor polar lipid accumulation

Table 1
Characterization by gas chromatography coupled with mass spectrometry of subcellar fractions obtained on a sucrose gradient by ultracentrifugation of cellular extracts of untreated and 7KC-treated U937 cells previously stained with MDC or NR

	MDC or NR negative fractions Sucrose gradient (fractions: 10–21% and 29–42%)	MDC or NR positive fractions Sucrose gradient (fractions: 22–28%)
Staining with MDC		
Untreated cells		
Sphingomyelin (pg/cell)	0.98±0.08	1.68±0.11
Phosphatidylcholin (pg/cell)	0.95±0.5	1.46±0.9
Cholesterol (pg/cell)	2.03±0.96	2.82±1.2
7KC (pg/cell)	0	0
7KC-treated cells		
Sphingomyelin (pg/cell)	1.1±0.8	10.21±0.4*
Phosphatidylcholin (pg/cell)	5.02±2.8	22.8±0.6*
Cholesterol (pg/cell)	2.5±0.5	58.4±0.2*
7KC (pg/cell)	1.96±0.7	74.4±1.2*
Staining with NR		
Untreated cells		
Sphingomyelin (pg/cell)	0.09±0.05	0.17±0.01
Phosphatidylcholin (pg/cell)	0.6±0.4	0.83±0.5
Cholesterol (pg/cell)	2.12±0.6	2.68±0.8
7KC (pg/cell)	0	0
7KC-treated cells		
Sphingomyelin (pg/cell)	0.9±0.14	1.92±0.2*
Phosphatidylcholin (pg/cell)	2.97±1.7	19.5±0.96*
Cholesterol (pg/cell)	2.2±0.7	82.8±10.1*
7KC (pg/cell)	1.68±1	204.9±20.4*

Cells were cultured in the presence or in the absence of 7KC (20 μg/ml) for 24 h and stained with MDC or NR used at 0.05 mM and 0.1 μg/ml, respectively. Data are mean±S.E. of three independent experiments. *P<.05, untreated vs. 7KC-treated cells.

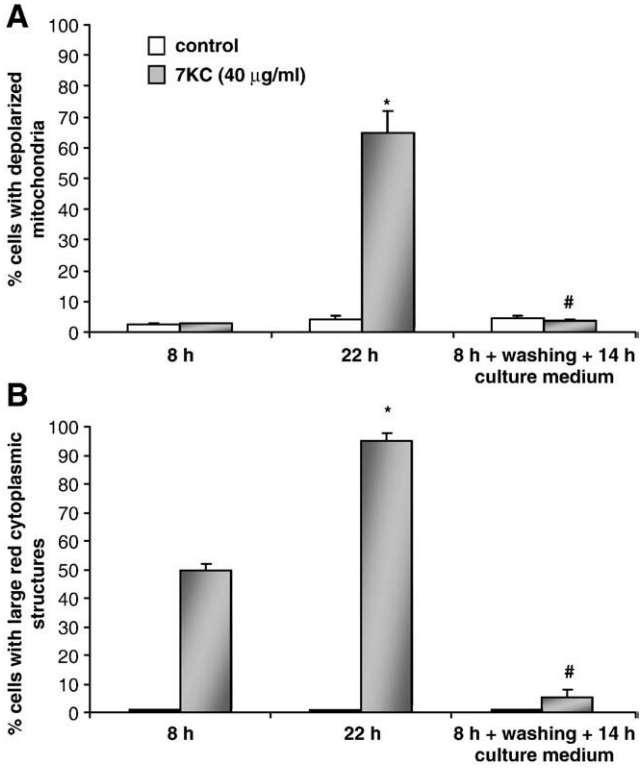

Fig. 2. Reversibility of 7KC-induced polar lipid accumulation. U937 cells were cultured in the absence or in the presence of 7KC (40 μg/ml; 100 μM) for 8, 22 or 8 h and further washed, and resuspended in culture medium for only 14 h. In these conditions, at 8 and 22 h, the percentages of cells with depolarized mitochondria corresponding to dead cells (A) and with large red cytoplasmic structures (above 630 nm) (B) were determined by staining with DiOC6(3) and NR (0.1 μg/ml), respectively. Data presented are means±S.E. of at least three independent experiments. *P<.05, untreated vs. 7KC-treated cells; #P<.05, 7KC-treated cells resuspended in culture medium vs. 7KC-treated cells.

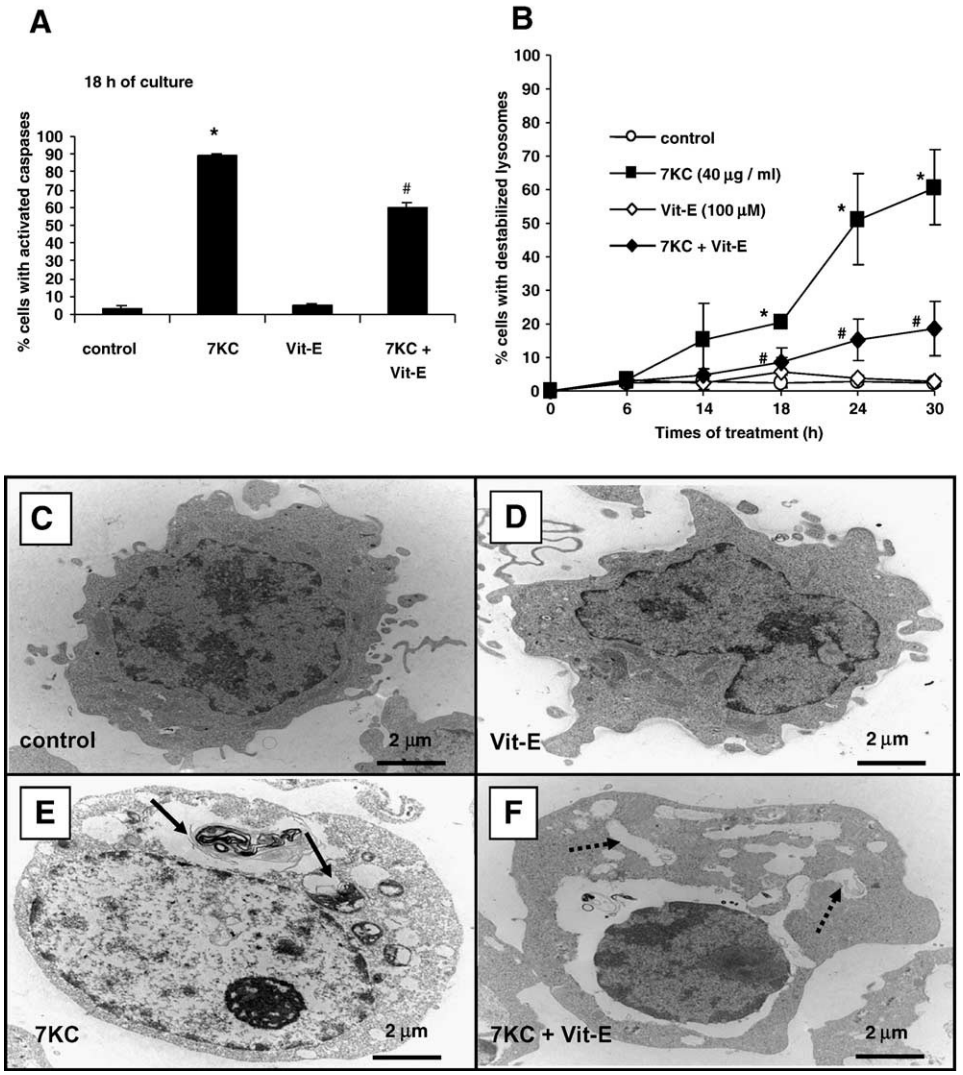

Fig. 3. Effects of Vit-E on caspase activation, lysosomal destabilization and myelin figure formation. U937 cells were cultured in the absence or presence of 7KC (40 µg/ml; 100 µM) for various periods of time (6, 14, 18, 24 and/or 30 h) and the effects of Vit-E (Vit-E, 100 µM) on apoptosis and on various cellular events associated with phospholipidosis were investigated. (A) In situ detection of activated caspases with FLICA in untreated or 7KC-treated cells cultured for 18 h in the absence or presence of Vit-E. (B) Effects of Vit-E on lysosomal destabilization evaluated by flow cytometry after staining with AO. Effects of Vit-E on myelin figure formation. (C) Untreated cells. (D) Vit-E-treated cells. (E) 7KC-treated cells. (F) 7KC+Vit-E-treated cells. Data presented are means±S.E. of at least three independent experiments. $^{*}P<.05$, untreated vs. 7KC-treated cells; $^{\#}P<.05$, 7KC-treated vs. 7KC+Vit-E-treated cells.

in atherosclerotic lesions [41,42], and they clearly establish the importance of 7KC in this process.

3.2. Impairment of 7KC induced phospholipidosis by Vit-E

Vit-E has been described as protecting against atherosclerosis [43], and we previously reported that this compound was able to reduce 7KC-induced cytosolic release of cytochrome *c*, overproduction of superoxide anions and the percentages of MDC-positive cells [11,18]. So, on U937 cells, we studied whether Vit-E (100 µM) was capable of impairing caspase activation measured by the in situ detection of activated caspases with FLICA, destabilization of lysosomes determined after staining with AO, myelin figure formation identified by transmission electron microscopy, accumulation of polar lipids evaluated after staining with NR and the lipid constitution and organization of the cytoplasmic membrane measured with MC540 (Figs. 3, 4). It is noteworthy that when Vit-E was added to the culture medium 30 min before treatment with 7KC (40 µg/ml), the percentages of U937 cells with activated caspases and with destabilized lysosomes were significantly reduced, and the formation of myelin figures was counteracted (Fig. 3). Thus, whereas large vacuoles, containing myelin figures, were observed in the cytoplasm of 7KC-treated cells (Fig. 3E), some vacuoles with small myelin figures or with no myelin figures were present in cells treated with 7KC in the presence of Vit-E (added 30 min before) (Fig. 3F). In addition, in 7KC-treated cells coincubated with Vit-E, the accumulation of polar lipids (red fluorescence of NR measured above 630 nm) was also strongly reduced as

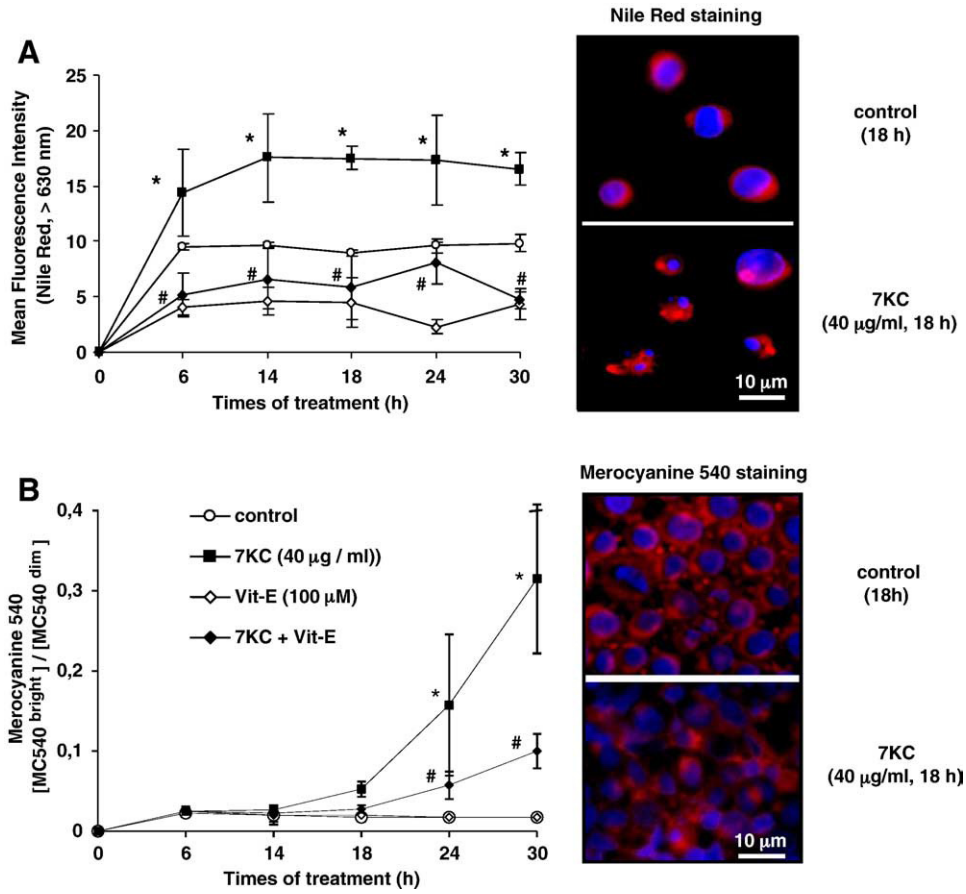

Fig. 4. Effects of Vit-E on polar lipid accumulation and cytoplasmic membrane organization. U937 cells were cultured in the absence or presence of 7KC (40 µg/ml; 100 µM) for various periods of time (6, 14, 18, 24 and 30 h) and the effects of Vit-E (100 µM) on cellular events associated with phospholipidosis were investigated. (A) Effects of Vit-E on polar lipid accumulation determined by flow cytometry after staining with NR. (B) Effects of Vit-E on the organization and lipid content of cytoplasmic membrane was determined by flow cytometry after staining with MC 540 by the [MC 540 bright cells]/[MC 540 dim cells] ratio. Data presented are means±S.E. of at least three independent experiments. *P<.05, untreated vs. 7KC-treated cells; #P<.05, 7KC-treated vs. 7KC+Vit-E-treated cells.

were the percentages of cells with disorganized cytoplasmic membranes resulting from qualitative, quantitative and/or altered packing of lipids evaluated with MC540 by the [MC 540 bright cells]/[MC 540 dim cells] ratio (Fig. 4). Taken together, these different data demonstrate that Vit-E is a potent inhibitor of 7KC-induced phospholipidosis.

3.3. Measurement of membrane fluidity by fluorescence anisotropy

Since the data obtained with MC540, in agreement with altered packing of lipids (disturbed membrane bilayer asymmetry previously shown by staining with annexin V) [44], do not contribute additional information at a molecular/biophysical level, fluorescence anisotropy was used to measure the effects of 7KC and Vit-E on membrane fluidity. Indeed, the presence of sterol in the plasma membrane has been shown to induce phase separations into distinct domains [45]. Moreover, the presence of sterols as cholesterol is known to lower the transition temperature between the gel and the lamellar fluid liquid crystalline phase of phospholipids [46]. Therefore, on U937 cells, we investigated whether 7KC induced a certain degree of plasma membrane rigidification and whether Vit-E was capable of counteracting these changes. In order to measure plasma membrane fluidity changes induced by 7KC and/or Vit-E, cells were grown for 18 h in presence of 7KC and/or Vit-E and then the membrane was labelled using the DPH hydrophobic probe. Changes in the lipid core of the plasma membrane were measured using anisotropy fluorescence (r) of DPH. This method provides data on the overall structure of the plasma membrane [47]. The results presented in Fig. 5 show that the mean r values of control cells (0.162±0.05) and Vit-E-treated cells (0.171±0.013) were similar, whereas the r values of 7KC (0.225±0.006) and (7KC+Vit-E)-treated cells (0.214±0.001) were significantly higher, as was the corresponding Δr. These observations led to the conclusion that (1) 7KC rigidified plasma membrane and (2) this rigidification was not prevented by Vit-E.

3.4. Impairment by Vit-E of the inactivation of the PI3-K/PDK-1/Akt signalling pathway associated with 7KC-induced apoptosis

Lipid second messengers, particularly those derived from the polyphosphoinositide cycle, play pivotal roles in several

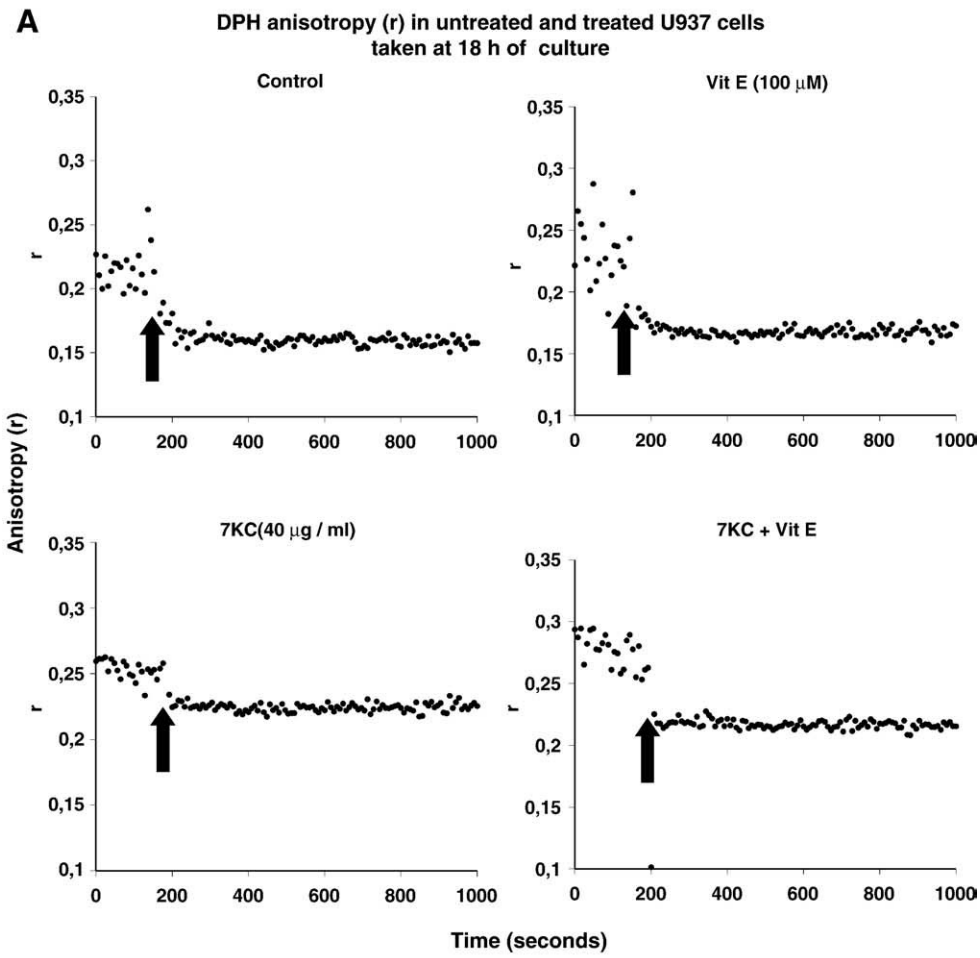

B Fluorescence anisotropy (r) values at 10 min after DPH incorporation in the plasma membrane of U937 cells taken at 18 h of culture

Treatments	Anisotropy (r)	Δr*
Control	*0.162 ± 0.005*	*0.000 ± 0.000*
7KC (40 μg/ml)	*0.225 ± 0.006 **	*0.063 ± 0.007*
Vit-E (100 μM)	*0.171 ± 0.013 **	*0.009 ± 0.020*
7KC+ Vit-E	*0.214 ± 0.001 **	*0.052 ± 0.004*

Δr* indicates the change in anisotropy recorded in treated cells relative to the control

Fig. 5. Effect of 7KC and Vit-E on plasma membrane fluidity. U937 cells were grown for 18 h in presence of 7-KC (40 μg/ml; 100 μM) and/or Vit-E (100 μM), washed and resuspended in PBS and labelled with DPH probe (1 μM). (A) Changes in DPH anisotropy with time. Each curve is a representative curve of qualitative and quantitative variations of r values. (B) Means of *r* values and Δ*r* recorded and calculated 10 min after addition of DPH to the cell suspension. The arrows indicate DPH incorporation time. Data presented are means±S.E. of three independent experiments. Differences between untreated (control) and 7KC, Vit-E and 7KC+Vit-E were analyzed by a Student *t* test. A *P* value of .05 or less was considered as statistically significant (*$P<.05$).

cell signalling networks. As 7KC-induced cell death is associated with numerous lipid modifications, those occurring at the cytoplasmic membrane level identified by staining with MC540 may contribute to inactivating the PI3-K/PDK-1/Akt signalling pathway, which is located on the inner cytoplasmic membrane and controls downstream signal transduction cascades involved in the regulation of the equilibrium between life and death. Thus, the effects of 7KC on PI3-K activity and on the phosphorylation of PDK-1 and Akt were investigated. In addition, as Vit-E was capable of impairing the lipid modifications occurring at the cytoplasmic membrane level, as shown by staining with MC540, the effects of Vit-E on PI3-K activity, as well as on the phosphorylation state of PDK-1 and Akt, were also studied.

Consequently, when U937 cells were cultured with 7KC (40 μg/ml) for 24 h, a substantial decrease in PI3-K activity was observed. Indeed, compared to untreated cells, the quantity of $PI(3,4,5)P_3$ per 10^6 cells was sharply reduced in 7KC-treated cells (Fig. 5A); it is known that $PI(3,4,5)P_3$ is the main product resulting from the enzymatic kinase activity of PI3-K on the substrate $PI(4,5)P_2$. Interestingly, significantly higher values of $PI(3,4,5)P_3$ were found when the cells were cultured in the presence of 7KC associated with Vit-E (Fig. 6A). Similarly, compared to untreated cells, lower levels of the PDK-1 and Akt kinases and their enzymatically active phosphorylated forms were found in 7KC-treated cells, and these effects were counteracted by Vit-E (Fig. 6B). Thus, Vit-E is capable of impairing the inactivation of the PI3-K/PDK-1/Akt signalling pathway associated with 7KC-induced apoptosis.

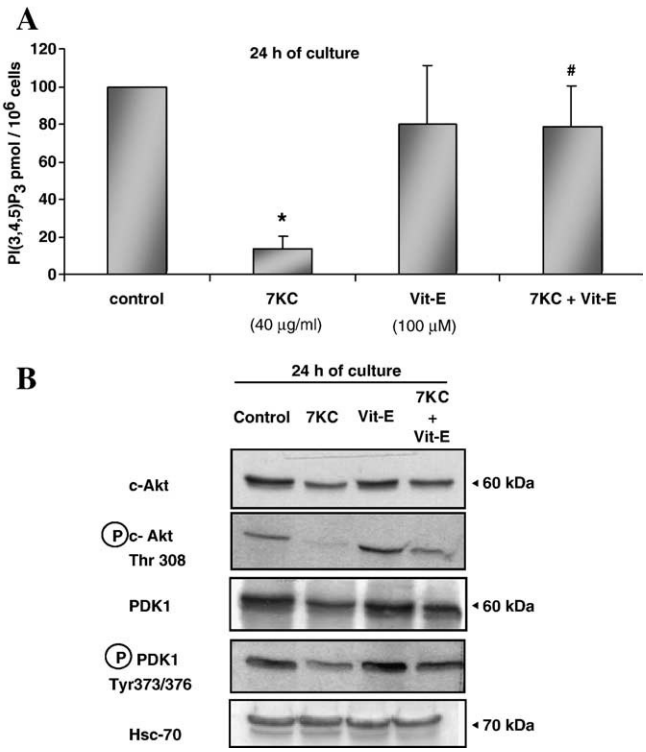

Fig. 6. Effects of Vit-E on PI3-K activity and on the content and phosphorylation of PDK-1 and Akt during 7KC-induced apoptosis. U937 cells were cultured in the absence or presence of 7KC (40 μg/ml; 100 μM) for 24 h and the effects of Vit-E (100 μM) on the different components of the PI3-K/PDK-1/Akt pathway were investigated. (A) Effects of Vit-E on PI3-K activity measured on cell extracts with the PIP_3 Mass ELISA kit (Echelon Biosciences). Data presented are means±S.E. of at least three independent experiments. $^{*}P<.05$, untreated vs. 7KC-treated cells; $^{\#}P<.05$, 7KC-treated vs. 7KC+Vit-E-treated cells. (B) Effects of Vit-E on PDK-1 and Akt content and phosphorylation were investigated by Western blot. At the end of the incubation time, cell extracts were collected, subjected to SDS-PAGE and immunoblotted with anti-Akt, anti-Akt phospho Thr 308, anti-PDK-1 and anti-PDK-1 phospho Tyr 373/376 antibodies. An anti-Hsc-70 monoclonal antibody was used to verify the regular expression of Hsc-70 used as internal standard. Data shown in (B) are representative of three independent experiments.

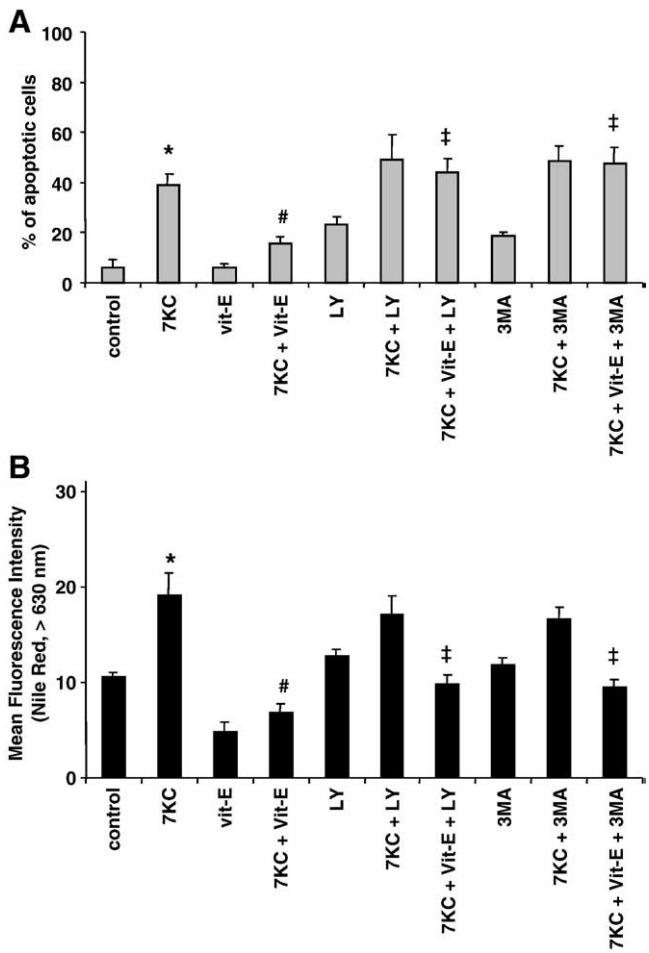

Fig. 7. Effects of two inhibitors of PI3-K (LY-294002, 3-methyladenine) on Vit-E activity. U937 cells were cultured in the absence or presence of 7KC (40 μg/ml; 100 μM) for 24 h and the effects of Vit-E (100 μM) and of inhibitors of PI3-K {LY-294002 [(LY), 40 μM; 3-methyladenine (3MA), 10 mM]} associated or not with Vit-E were evaluated using fluorescence microscopy after staining with Hoechst 33342, which identifies apoptotic cells (A) and by flow cytometry after staining with NR, which evaluates polar lipid accumulation (B). Data presented are means±S.E. of at least three independent experiments. $^{*}P<.05$, untreated vs. 7KC-treated cells; $^{\#}P<.05$, 7KC-treated vs. 7KC+Vit-E-treated cells; $^{\ddagger}P<.05$, 7KC+Vit-E-treated vs. [7KC+Vit-E+LY (or 3MA)]-treated cells.

3.5. Effects of PI3-K inhibitors on the activity of Vit-E

In order to specify the role played by PI3-K on the protective effects of Vit-E on 7KC-induced apoptosis and polar lipid accumulation, two inhibitors of this kinase were used: LY-294002 and 3-methyladenine (3MA). Thus, Vit-E was associated with these inhibitors to determine the role of PI3-K on its protective effects. LY-294002 was used at 40 μM, and 3 MA at 10 mM, which are concentrations reported to inhibit the PI3-K/Akt signalling pathway [48,49]. At this concentration, LY-294002 and 3MA slightly enhance apoptosis (Fig. 7). When LY-294002 and 3MA were associated with 7KC, no significant effects were observed on 7KC-induced apoptosis and polar lipid accumulation (Fig. 7). However, when LY-294002 and 3MA were

associated with Vit-E, they impaired its ability to counteract apoptosis and to reduce polar lipid accumulation (Fig. 7). These findings support the argument that Vit-E positively regulates PI3-K activity, playing key roles in the control of 7KC-induced apoptosis and also involved in the regulation of polar lipid metabolism.

4. Discussion

Given the considerable accumulation of oxysterols in atherosclerotic plaques and their ability to induce a complex mode of cell death associated with some characteristics of apoptosis [50] as well as with overproduction of reactive oxygen species [5] and cytokine secretion [6], which are hallmarks of the atherosclerotic process, it is important to identify the cellular events and the metabolic pathways associated with the different biological effects triggered by these cholesterol oxide derivatives. To this end, human U937 promonocytic leukaemia cells were treated with 7KC used in the range of levels measured in the plasma of patients after a fat-rich meal [51] and of cholesterol-rich fed rabbit [52]. U937 cells were chosen because they are sensitive to oxysterols in the same range of concentrations as those observed on the cells of the vascular wall (endothelial and smooth muscle cells) [53]. In addition, U937 cells are frequently used as macrophage-like reference models to investigate the cytotoxic activities of oxysterols because it is well accepted that macrophages play an important role in atherosclerotic process [54].

Under these conditions, we demonstrated that 7KC-induced apoptosis is associated with considerable cytoplasmic modifications, including a reversible formation of multilamellar structures that we previously called myelin figures [11], which are polar lipid-rich structures, containing high levels of phosphatidylcholine and sphingomyelin, and localized in acidic compartments. Interestingly, these different features are the pathologic and morphologic characteristics of phospholipidosis defined by the following criteria: ultrastructural appearance of membranous lamellar inclusions (also called lysosomal inclusion bodies or myeloid bodies); excessive accumulation of phospholipids in cells, predominantly lysosomal in origin and reversibility of alterations after discontinuance of drug treatment [20,21]. Until now, phospholipidosis has never been described with oxysterol treatment, and the main in vivo and in vitro reports concern phospholipidosis induced by drugs with cationic amphiphilic structures such as amiodarone, fluoxetine, imipramine, chlorcyclizine, tamoxifen and gentamicin [20]. At the moment, drug-induced phospholipidosis remains an unresolved problem because the molecular causes are unclear, and its relationships with various cytotoxic effects, including the induction of cell death, are not well known. It has been suggested that phospholipidosis might be a part of a defense mechanism when the cell is confronted with a substantial accumulation of xenobiotics and their metabolites because the presence of multilamellar structures in acidic compartments might favour the inactivation of cytotoxic compounds [20,21]. In addition, multilamellar bodies have been observed to undergo exocytosis and therefore might contribute to reducing accumulation of cytotoxic molecules [21]. However, observations also support the notion that phospholipidosis might be a part of cell death. Indeed, amiodarone and imipramine, which are two major inducers of phospholipidosis, were also shown to inhibit cell proliferation and to activate caspase-mediated apoptosis in cell culture [55]. Moreover, in murine macrophages loaded with free cholesterol, some phospholipid whorls, suggesting myelin figures, have been observed, and their presence is associated with considerable cytotoxic effects, including a stress of the reticulum connected with the induction of a mode of cell death by apoptosis [56]. It has also been suggested that the rupture of the acidic compartments containing multilamellar structures might release some proteolytic enzymes in the cytoplasm [21], which might subsequently contribute to activating certain apoptotic pathways. During 7KC-induced cell death, this possibility is supported by the destabilization of lysosomes observed by staining with AO and by the ability to inhibit 7KC- and 7β-hydroxycholesterol-induced apoptosis with inhibitors of cathepsin B and L [57]. Therefore, our different observations argue in favour of the hypothesis that phospholipidosis might play key roles in the induction of 7KC-induced cell death. By analogy with lipoapoptosis, which is a mode of cell death resulting from the accumulation of long-chain fatty acids inside the cells [58], phospholipidosis might be a mode of cell death resulting from the cytoplasmic accumulation of phospholipids. In addition, the important roles of phospholipids during apoptosis have also been established at the cytoplasmic membrane level. Indeed, the spatial organization of membrane lipids is crucial, and the externalization of phosphatidylserine on the outer leaflet of the cytoplasmic membrane is recognized as a key and early event of the apoptotic process [59]. Since 7KC-induced cell death is also associated with a rapid externalization of phosphatidylserine [42], and since our data obtained with merocyanine 540 underline that 7KC contributes to disorganizing the packaging of cytoplasmic membrane lipids, these observations resulted in specifying the effects of 7KC on the PI3-K/PDK-1/Akt signalling pathway, which is closely associated with the cytoplasmic membrane and is involved in the control of some life and death signals [15].

Thus, in agreement with data obtained on 7KC-treated murine P388D1 macrophages [19], Akt degradation is observed, and this is associated with an absence of phosphorylation on threonine 308, which is required for Akt activity, as demonstrated by mutagenesis studies [60]. Consequently, certain signalling pathways involved in cell death are disturbed. One of them is the regulation of signalling via the nuclear factor-κB (NF-κB) transcription factor pathway. Usually, NF-κB is maintained in the cytoplasm as an inactive complex via its inhibitor IκB, and

when Akt is activated, it phosphorylates IκB, which is degraded, thus allowing the migration of NF-κB into the nucleus to transactivate numerous genes involved in cell proliferation such as $p27^{kip1}$ or glycogene synthetase kinase 3 (GSK3) [61]. It is also known that Akt in its active form sequesters the proapoptotic form of the BAD protein into the cytoplasm and reduces the activity of caspase-9 [15], which are two important proteins involved in 7KC-induced apoptosis [17,61]. Therefore, in agreement with previous investigations, inhibition of Akt activity constitutes a major premitochondrial event involved in 7KC-induced cell death.

Based on the diversity and on the complexity of the mechanisms capable of contributing to the dephosphorylation of Akt, involving both kinases and phosphatases, we chose to specify the role played by the PI3-K for the following reasons: this kinase leads to the synthesis of PI(3,4,5)P_3; this inositol is necessary for PDK-1 recruitment and activity, which can, in turn, phosphorylate Akt on threonine 308 [15]. The lower level of PI(3,4,5)P_3 observed in 7KC-treated cells and the degradation of PDK-1 associated with an absence of phosphorylation on Thyrosine 373 and 376 mean that the loss of PI3-K activity constitutes an important initial event, subsequently leading to the inactivation of PDK-1 and of Akt. However, some other enzymes may also contribute to this process. Thus, with 7KC treatment, we cannot exclude an activation of the phosphatase and tensin homologue deleted on chromosome 10, reverting the formation of PI(3,4,5)P_3 into PI(4,5)P_2, and/or an activation of the phosphatase-2A (PP2A) protein, which dephosphorylates PDK-1 and Akt and might therefore also contribute to decreasing Akt activity [15,60,61].

Whether or not there is a link between PI3-K/PDK-1/Akt signalling pathway, accumulation of sphingomyelin and phosphatidylcholine is questionable. Based on previous investigations, accumulation of sphingomyelin can be attributed to the ability of 7KC to inhibit sphingomyelinase [62] and can therefore occur independently of the PI3-K/PDK-1/Akt signalling pathway. As for phosphatidylcholine, since free cholesterol accumulation occurring with 7KC treatment [28] has been shown to involve stimulation of CTP — phosphocholine cytidylyltransferase through partial dephosphorylation of membrane-bound CT — similar effects have been suggested on other proteins [63]. Thus, a possible link with PI3-K/PDK-1/Akt activity cannot be excluded, and the ability of the PI3-K inhibitors [LY-294002 or 3-methyladenine (3MA)] to favour the accumulation of polar lipids supports this hypothesis. In addition, if we assume that the important cytoplasmic accumulation of sphingomyelin and phosphatidylcholine is associated with a decrease in these phospholipids in lipid rafts, which are phospholipid-rich domains playing key roles in signal transduction [64], this might also contribute to changing specific lipid–protein interactions and modifying important signalling cascades such as the PI3-K/PDK-1/Akt signalling pathway.

Moreover, since Vit-E (α-tocopherol) (in addition to its anti-oxidative properties [65]) has the ability (1) to regulate gene expression and to act on some signalling pathways [66,67], (2) to counteract 7KC-induced apoptosis [18], (3) to reduce the accumulation of MDC [11], which is associated with 7KC-induced phospholipidosis and (4) to interfere with phospholipid metabolism [68], it was necessary to specify its effects on phospholipidosis and the PI3-K/PDK-1/Akt signalling pathway. Until now, with known inducers of phospholipidosis such as amiodarone and desethylamiodarone, Vit-E has been shown to reduce the accumulation of these drugs and to counteract phospholipidosis biochemically evaluated by decreased cytoplasmic levels of phospholipids [69,70]. Our data contribute additional information to these reports. They show that the decreased accumulation of phospholipids is associated with an inhibition of myelin

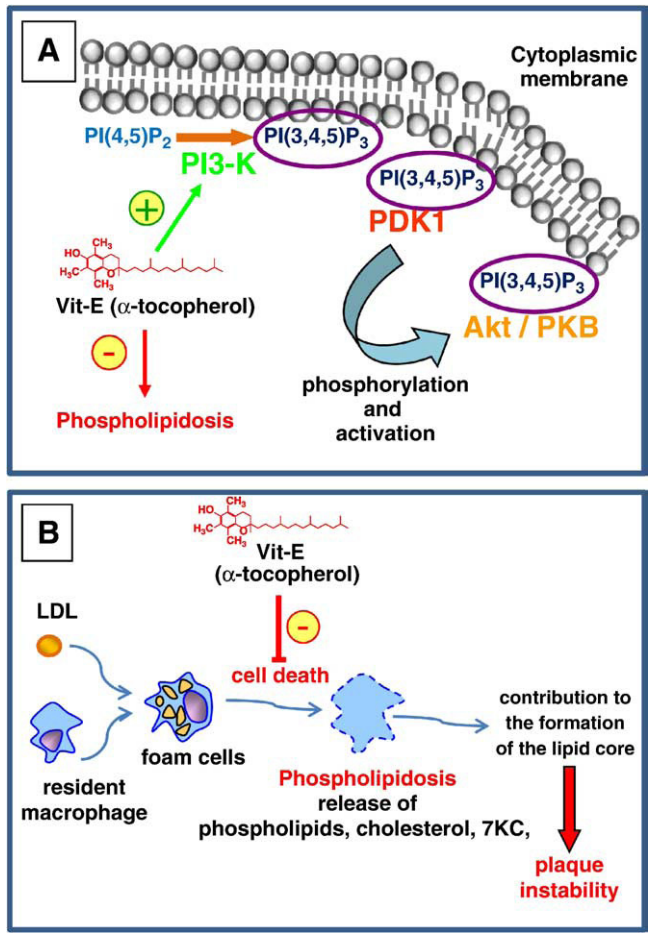

Fig. 8. Proposed model for the different effects of 7KC and Vit-E at the cellular level and on the development of atherosclerotic plaque. (A) At the cellular level, 7KC leads to decreased PI3-K activity, which contributes to reducing the level of PI(3,4,5)P_3 on the inner side of the cytoplasmic membrane. Consequently, PDK-1 activity decreases and cannot phosphorylate Akt/PKB. Moreover, 7KC leads to an increased cytoplasmic accumulation of polar lipids, contributing to phospholipidosis. These different side effects are counteracted by Vit-E. (B) At the vascular wall, the ability of Vit-E to counteract 7KC-induced cell death and consequently to reduce the release of the cellular component from dying cells (phospholipids, cholesterol, oxysterols, etc.) in the arterial wall might contribute to diminishing the lipid core and therefore to reducing plaque instability.

figure formation, whereas large vacuoles are still present. Therefore, they demonstrate, for the first, time the ability to dissociate the formation of multilamellar structures from those of acidic vacuoles. Consequently, this observation contributes to different hypotheses: Vit-E might inhibit the accumulation of phospholipids in the vacuoles, Vit-E might stimulate the degradation or inhibit the synthesis of phospholipids inside the vacuoles and/or Vit-E might re-establish the traffic of phospholipids towards other cell compartments, such as the endoplasmic reticulum or the plasma membrane. Thus, the ability of Vit-E to act on phospholipid content and distribution and on key enzymes of phospholipid metabolism such as PP2A [70,71] might at least partially explain its ability to restore the activity of the PI3-K/PDK-1/Akt signalling pathway in 7KC-treated cells. However, the inability of Vit-E to restore membrane fluidity, demonstrated by fluorescence anisotropy, suggests that its positive effects would concern only minor and particular domains of the cytoplasmic membrane, such as those involved in signal transduction defined as raft microdomains. Indeed, as 7KC accumulates in lipid rafts [17], Vit-E might counteract the accumulation of this oxysterol in these microdomains and consequently contribute to restoring cell viability [72]. Interestingly, as inhibition of polar lipid accumulation was less efficient when Vit-E was associated with PI3-K inhibitors (LY-294002or 3MA), our data support a role of PI3-K in polar lipid metabolism, and the ability of these inhibitors to counteract the protective effects of Vit-E on 7KC-induced apoptosis clearly establishes that Vit-E positively regulates PI3-K and that the signals activated by Vit-E are located upstream from PI3-K. According to the different data obtained in the present study, we have proposed a model that summarizes the effects of Vit-E at the cellular level to prevent 7KC-induced cell death as well as polar lipid accumulation, and at the vascular level to impair the development of atherosclerotic plaque (Fig. 8). It is noteworthy that whereas the potential benefits of Vit-E in atherosclerosis are not clearly established despite numerous demonstrations of beneficial effects in vitro and in animal studies, the factors involved in the failure of Vit-E therapy are beginning to be identified [73]. They not only include extrinsic factors, such as diet and lifestyle, but also intrinsic factors such as the polymorphism of p22(phox) related to the plasma level of Vit-E [74] or the ability of phospholipid transfer protein to distribute Vit-E in the tissues [75]. Therefore, in clinical practice in the future, we can assume that better patient characterization will probably contribute to identifying the beneficial effects of Vit-E in humans.

In conclusion, whereas U937 cells are tumoral cells, it has been previously reported that the mode of cell death induced by 7KC on these cells shares similarities with the cell death process observed on the cells of the vascular wall [76,77]. Therefore, we can consider that the analysis of 7KC-induced phospholipidosis contributes new information on the cellular changes and the metabolic pathways triggered by this oxysterol. Interestingly, the involvement of phospholipidosis reveals a number of relationships between cell death and the metabolism, distribution, and trafficking of phospholipids, which are known to modulate numerous signalling pathways such as those involved in the control of the equilibrium between life and death. Moreover, the ability of Vit-E to inhibit phospholipidosis and to counteract important lipid changes occurring at various cellular levels treated by 7KC, such as the inactivation of the PI3-K/PDK-1/Akt signalling pathway, not only underscores the anti-atherosclerotic properties of Vit-E but also highlight potential pharmacological cellular targets which might be of interest to prevent and/or treat particular forms of atherosclerosis associated with major phospholipid disorders.

Acknowledgments

This work was supported by grants from the Inserm, the Ligue Contre Le Cancer (Comité de Côte d'Or) and the Conseil Régional de Bourgogne. We thank Mr Franck Ménétrier (Laboratoire de Microscopie, Inserm IFR STIC-Santé, Dijon, France) for his technical support in electron microscopy. We also acknowledge Ms Jeannine Lherminier (Service Commun de Microscopie Electronique, INRA, Dijon, France) for the observations by transmission electron microscopy, Profs Yves Wache and Jean-Marie Perrier-Cornet [Plateau Imagerie-Spectroscopie (IFR 92) — ENSBANA, Dijon, France], Ms Lucy Martine (INRA, Groupe Vision et Nutrition, UMR 1129 FLAVIC, Dijon, France) for the analyses of cholesterol and 7KC by capillary gas chromatography and Ms Anne Athias (Inserm IFR STIC-Santé/plateau technique lipidomique, Dijon, France) for the analyses of phospholipids by gas chromatography coupled with mass spectrometry. The authors are also indebted to Ms Linda Northrup for reviewing the English version of the manuscript.

References

[1] Smith L. Review of progress in sterol oxidations: 1987-1995. Lipids 1996;31:453–7.
[2] Colles SM, Maxson JM, Carlson SG, Chilsolm GM. Oxidized LDL-induced injury and apoptosis in atherosclerosis. Trends Cardiovasc Med 2001;11:131–8.
[3] Schroepfer GJ. Oxysterols: modulators of cholesterol metabolism and other processes. Physiol Rev 2000;80:361–554.
[4] Diczfalusy U. Analysis of cholesterol oxidation products in biological samples. J AOAC Int 2004;87:467–73.
[5] Lemaire-Ewing S, Prunet C, Montange T, Vejux A, Berthier A, Bessède G, et al. Comparison of the cytotoxic, pro-oxidant and pro-inflammatory characteristics of different oxysterols. Cell Biol Toxicol 2005;21:97–114.
[6] Prunet C, Montange T, Véjux A, Laubriet A, Rohmer JF, Riedinger JM, et al. Multiplexed flow cytometric analyses of pro- and anti-inflammatory cytokines in the culture media of oxysterol-treated human monocytic cells and in the sera of atherosclerotic patients. Cytometry A 2006;69:359–73.
[7] Tedgui A, Mallat Z. Cytokines in atherosclerosis: pathogenic and regulatory pathways. Physiol Rev 2006;86:515–81.
[8] Vejux A, Kahn E, Ménétrier F, Montange T, Lherminier J, Riedinger JM, et al. Cytotoxic oxysterols induce caspase-independent myelin

figure formation and caspase-dependent polar lipid accumulation. Histochem Cell Biol 2007;127:609–24.
[9] Kahn E, Vejux A, Lizard G, Bessède G, Frouin F, Prunet C, et al. Analysis of the fluorescence of monodansylcadaverine-positive cytoplasmic structures during 7-ketocholesterol-induced cell death. Anal Quant Cytol Histol 2004;26:47–56.
[10] Hariri M, Millane G, Guimond MP, Guay G, Dennis JW, Nabi IR. Biogenesis of multilamellar bodies via autophagy. Mol Biol Cell 2000; 11:255–68.
[11] Miguet-Alfonsi C, Prunet C, Monier S, Bessède G, Lemaire-Ewing S, Berthier A, et al. Analysis of oxidative processes and of myelin figure formation before and after the loss of mitochondrial potential during 7b-hydroxycholesterol and 7-ketocholesterol-induced apoptosis: comparison with various pro-apoptotic chemicals. Biochem Pharmacol 2002;64:527–41.
[12] Martinet W, De Bie M, Schrijvers DM, De Meyer GR, Herman AG, Kockx MM. 7-ketocholesterol induces protein ubiquitination, myelin figure formation, and light chain 3 processing in vascular smooth muscle cells. Arterioscler Thromb Vasc Biol 2004;24: 2296–301.
[13] Bauvy C, Gane P, Arico S, Codogno P, Ogier-Denis E. Autophagy delays sulindac sulfide-induced apoptosis in the human intestinal colon cancer cell line HT-29. Exp Cell Res 2001;268:139–49.
[14] Petiot A, Ogier-Denis E, Blommaart EF, Meijer AJ, Codogno P. Distinct classes of phosphatidylinositol 3¢-kinases are involved in signaling pathways that control macro-autophagy in HT-29 cells. J Biol Chem 2000;275:992–8.
[15] Datta SR, Brunet A, Greenberg ME. Cellular survival: a play in three Akts. Gene Dev 1999;13:2905–27.
[16] Neri LM, Borgatti P, Capitani S, Martelli AM. The nuclear phosphoinositide 3-kinase/Akt pathway: a new second messenger system. Biochim Biophys Acta 2002;1584:73–80.
[17] Berthier A, Lemaire-Ewing S, Prunet C, Monier S, Athias A, Bessède G, et al. Involvement of a calcium-dependent dephosphorylation of BAD associated with the localization of Trpc-1 within lipid rafts in 7-ketocholesterol-induced THP-1 cell apoptosis. Cell Death Differ 2004;11:897–905.
[18] Lizard G, Miguet C, Bessède G, Monier S, Gueldry S, Néel D, et al. Impairment with various antioxidants of the loss of mitochondrial transmembrane potential and of the cytosolic release of cytochrome *c* occurring during 7-ketocholesterol-induced apoptosis. Free Radic Biol Med 2000;28:743–53.
[19] Rusinol AE, Thewke D, Liu J, Freeman N, Panini SR, Sinensky MS. AKT/protein kinase B regulation of BCL family members during oxysterol-induced apoptosis. J Biol Chem 2004;279:1392–9.
[20] Reasor MJ, Kacew S. Drug-induced phospholipidosis: are there functional consequences? Exp Biol Med 2001;226:825–30.
[21] Anderson N, Borlak J. Drug-induced phospholipidosis. FEBS Lett 2006;580:5533–40.
[22] Blommaart EFC, Luiken JJFP, Meijer AJ. Autophagic proteolysis: control and specificity. Histochem J 1997;29:365–85.
[23] Grabarek J, Amstad P, Darzynkiewicz Z. Use of fluorescently labeled caspase inhibitors as affinity labels to detect activated caspases. Hum Cell 2002;15:1–12.
[24] Vejux A, Lizard G, Tourneur Y, Riedinger JM, Frouin F, Kahn E. Effects of caspase inhibitors (z-VAD-fmk, z-VDVAD-fmk) on Nile Red fluorescence pattern in 7-ketocholesterol-treated cells: investigation by flow cytometry and spectral imaging microscopy. Cytometry A 2007;71:550–62.
[25] Lizard G, Fournel S, Genestier L, Dhedin N, Chaput C, Flacher M, et al. Kinetics of plasma membrane and mitochondrial alterations in cells undergoing apoptosis. Cytometry 1995;21:275–83.
[26] Biederbick A, Kern HF, Elsässer HP. Monodansylcadaverine (MDC) is a specific in vivo marker for autophagic vacuoles. Eur J Cell Biol 1995; 66:3–14.
[27] Klinkner AM, Bugelski PJ, Waites R, Louden C, Hart TK, Kerns WD. A novel technique for mapping the lipid composition of atherosclerotic fatty streaks by en face fluorescence microscopy. J Histochem Cytochem 1997;45:743–53.
[28] Vejux A, Kahn E, Dumas D, Bessède G, Ménétrier F, Athias A, et al. 7-Ketocholesterol favors lipid accumulation and colocalizes with Nile Red positive cytoplasmic structures formed during 7-ketocholesterol-induced apoptosis: analysis by flow cytometry, FRET biphoton spectral imaging microscopy, and subcellular fractionation. Cytometry A 2005;64:87–100.
[29] Schlegel RA, Stevens M, Lumley-Sapanski K, Williamson P. Altered lipid packing identifies apoptotic cells. Immunol Lett 1993;36:283–8.
[30] Laakko T, King L, Fraker P. Versatility of merocyanine 540 for the flow cytometric detection of apoptosis in human and murine cells. J Immunol Methods 2002;61:129–39.
[31] Ball RY, Carpenter KLH, Mitchinson MJ. Ceroid accumulation by murine peritoneal macrophages exposed to artificial lipoproteins: ultrastructural observations. Br J Exp Pathol 1988;69:43–56.
[32] Harman D. Lipofuscin and ceroid formation: the cellular recycling system. In: Porta EA, editor. Lipofuscin and Ceroid Pigments. New York: Plenum Press; 1990. p. 3–15.
[33] Olsson GM, Rungby J, Rundquist I, Brunk UT. Evaluation of lysosomal stability in living culture macrophages by cytofluorometry. Effect of silver lactate and hypotonic solutions. Virchows Arch - B: Cell Pathol 1989;56:263–9.
[34] Yuan XM, Li W, Brunk UT, Dalen H, Chang YH, Sevanian A. Lysosomal destabilisation during macrophage damage induced by cholesterol oxidation products. Free Radic Biol Med 2000;28: 208–18.
[35] Van Ginkel G, van Langen H, Levine YK. The membrane fluidity concept revised by polarized fluorescence spectroscopy on different models membranes containing unsaturated lipids and sterols. Biochimie 1989;71:23–32.
[36] Folch J, Lees M, Sloane Stanley GH. A simple method for the isolation and purification of total lipids from animal tissues. J Biol Chem 1957; 226:497–509.
[37] Becart I, Chevalier C, Biesse JP. Quantitative analysis of phospholipids by HPLC with a light scattering evaporating detector: application to raw materials for cosmetic use. J High Resolut Chromatogr 1990;13: 126–9.
[38] Smith PK, Krohn RI, Hermanson GT, Mallia AK, Gartner FH, Provenzano MD, et al. Measurement of protein using bicinchoninic acid. Anal Biochem 1985;150:76–85.
[39] Györkey F, Shimamura T, O'Neal R. The fine structure of ceroid in human atheroma. J Histochem Cytochem 1968;15:732–6.
[40] Kroemer G, Petit P, Zamzami N, Vayssière JL, Mignotte B. The biochemistry of programmed cell death. FASEB J 1995;9:1277–87.
[41] Shore NL, Zilversmit DB, Ackerman RF. Plasma phospholipid deposition in human serum and atherosclerotic lesions. Am J Physiol 1995;181:527–31.
[42] Kummerow FA, Cook LS, Wasowicz E, Jelen H. Changes in the phospholipid composition of the arterial cell can result in severe atherosclerotic lesions. J Nutr Biochem 2001;12:602–7.
[43] Bron D, Amis R. Vitamin E and the prevention of atherosclerosis. Int J Vitam Nutr Res 2001;71:18–24.
[44] Kahn E, Lizard G, Frouin F, Bernengo JC, Souchier C, Bessède G, et al. Confocal analysis of phosphatidylserine externalization with the use of biotinylated annexin V revealed with streptavidin FITC, -europium, -phycoerythrin or -Texas Red in oxysterol-treated apoptotic cells. Anal Quant Cytol Histol 2001;23:47–55.
[45] Stanley DW. Biological membrane deterioration and associated quality losses in food tissues. Crit Rev Food Sci Nutr 1991;30:487–6053.
[46] Chapman D. Phase transitions and fluidity characteristics of lipids and cell membranes. Q Rev Biophys 1975;8:185–235.
[47] Mely-Goubert B, Freedman MH. Lipid fluidity and membrane protein monitoring using 1,6-diphenyl-1,3,5-hexatriene. Biochim Biophys Acta 1980;601:315–27.
[48] Arico S, Petiot A, Bauvy C, Dubbelhuis PF, Meijer AJ, Codogno P, et al. The tumor suppressor PTEN positively regulates macroautophagy

by inhibiting the phosphatidylinositol 3-kinase/protein kinase B pathway. J Biol Chem 2001;276:35243–6.
[49] Uddin S, Hussain AR, Al-Hussein KA, Manogaran P, Wickrema A, Gutierriez MI, et al. Inhibition of phosphatidylinositol 3¢-kinase/AKT signaling promotes apoptosis of primary effusion lymphoma cells. Clin Cancer Res 2005;11:3102–8.
[50] Prunet C, Lemaire-Ewing S, Ménétrier F, Néel D, Lizard G. Activation of caspase-3 dependent and independent pathways during 7-ketocholesterol- and 7b-hydroxycholesterol-induced cell death: a morphological and biochemical study. J Biochem Mol Toxicol 2005;19:311–26.
[51] Emanuel HA, Hassel CA, Addis PB, Bergmann SD, Zavoral JH. Plasma cholesterol oxidation products (oxysterols) in human subjects fed a meal rich in oxysterols. J Food Sci 1991;56:843–7.
[52] Vine F, Mamo JCL, Beilin LJ, Mori TA, Croft KD. Dietary oxysterols are involved in plasma triglyceride rich lipoproteins, increase their susceptibility to oxidation and increase aortic cholesterol concentration in rabbits. J Lipid Res 1998;39:1995–2004.
[53] Lizard G, Monier S, Cordelet C, Gesquière L, Deckert V, Gueldry S, et al. Characterization and comparison of the mode of cell death, apoptosis versus necrosis, induced by 7b-hydroxycholesterol and 7-ketocholesterol in the cells of the vascular wall. Arterioscler Thromb Vasc Biol 1999;19:1190–200.
[54] Stoll G, Bendszus M. Inflammation and atherosclerosis: novel insight into plaque formation and destabilization. Stroke 2006;37:1923–32.
[55] Piccotti JR, LaGattuta MS, Knight SA, Gonzales AJ, Bleavins MR. Induction of apoptosis by cationic amphiphilic drugs amiodarone and imipramine. Drug Chem Toxicol 2005;28:117–33.
[56] Feng B, Yao PM, Li Y, Devlin CM, Zhang D, Harding HP, et al. The endoplasmic reticulum is the site of cholesterol-induced cytotoxicity in macrophages. Nat Cell Biol 2003;5:781–92.
[57] Li W, Dalen H, Eaton JW, Yuan XM. Apoptotic death of inflammatory cells in human atheroma. Arterioscler Thromb Vasc Biol 2001;21: 1124–30.
[58] Unger RH, Orci L. Lipoapoptosis: its mechanism and its diseases. Biochim Biophys Acta 2002;15:202–12.
[59] Koopman G, Reutelingsperger CPM, Kuijten GAM, Keehnen RMJ, Pals ST, van Oers MHJ. Annexin V for flow cytometric detection of phosphatidylserine expression on B cells undergoing apoptosis. Blood 1994;84:1415–20.
[60] Alessi DR, Caudwell FBN, Andjelkovic M, Hemmings BA, Cohen P. Molecular basis for the substrate specificity of protein kinase B; comparison with MAP kinase-1 and p70 S6 kinase. FEBS Lett 1996; 399:333–8.
[61] Hill MM, Hemmings BA. Inhibition of protein kinase B/Akt: implication for cancer therapy. Pharmacol Ther 2002;93:243–51.
[62] Maor I, Mandel H, Aviram M. Macrophage uptake of oxidized LDL inhibits lysosomal sphingomyelinase, thus causing the accumulation of unesterified cholesterol-sphingomyelin-rich particles in the lysosomes. A possible role for 7-ketocholesterol. J Lipid Res 1995;15: 1378–87.
[63] Shiratori Y, Houweling M, Zha X, Tabas I. Stimulation of CTP: phosphocholine cytidylyltransferase by free cholesterol loading of macrophages involves signaling through protein dephosphorylation. J Biol Chem 1995;270:29894–903.
[64] Simons K, Toomre D. Lipid rafts and signal transduction. Nat rev 2000;1:31–41.
[65] Singh U, Devaraj S, Jialal I. Vitamin E, oxidative stress, and inflammation. Annu Rev Nutr 2005;25:151–74.
[66] Azzi A, Gysin R, Kempna P, Munteanu A, Villacorta L, Visarius T, et al. Vitamin E mediates cell signaling and regulation of gene expression. Ann N Y Acad Sci 2004;1031:86–95.
[67] Zingg JM, Azzi A. Non-oxidant activities of Vitamin E. Curr Med Chem 2004;11:1113–33.
[68] Miguet C, Monier S, Bettaieb A, Athias A, Bessède G, Laubriet A, et al. Ceramide generation occurring during 7b-hydroxycholesterol- and 7-ketocholesterol-induced apoptosis is caspase independent and is not required to trigger cell death. Cell Death Differ 2001;8:83–99.
[69] Lucy JA. Structural interactions between vitamin E and polyunsaturated lipids. World Rev Nutr Diet 1978;31:184–9.
[70] Honegger UE, Scuntaro I, Wiesman UN. Vitamin E reduces accumulation of amiodarone and desethylamiodarone and inhibits phospholipidosis in cultured human cells. Biochem Pharmacol 1995; 49:1741–5.
[71] Yin KJ, Hsu CY, Hu XY, Chen H, Chen SW, Xu J, et al. Protein phosphatase 2A regulates bim expression via the Akt/FKHRL1 signaling pathway in amyloid-beta peptide-induced cerebrovascular endothelial cell death. J Neurosci 2006;26:2290–9.
[72] Cuschieri J, Bulger E, Biligren J, Garcia I, Maier RV. Vitamin E inhibits endotoxin-mediated transport of phosphatases to lipid rafts. Shock 2007;27:19–24.
[73] Richardson JA, Amantea CM, Kianmahd B, Tetradis S, Lieberman JR, Hahn TJ, et al. Oxysterol-induced osteoblastic differentiation of pluripotent mesenchymal cells is mediated through a PKC- and PKA-dependent pathway. J Cell Biochem 2007;100:1131–45.
[74] He MA, Cheng LX, Jiang CZ, Zeng HS, Wang J, Wang F, et al. Association of polymorphism of P22(phox) C242T, plasma levels of Vitamin E, and smoking with coronary heart disease in China. Am Heart J 2007;153:640–6.
[75] Schneider M, Vergès B, Klein A, Miller ER, Deckert V, Desrumaux C, et al. Alterations in plasma vitamin E distribution in type 2 diabetic patients with elevated plasma phospholipid transfer protein activity. Diabetes 2004;53:2633–9.
[76] Lizard G, Moisant M, Cordelet C, Monier S, Gambert P, Lagrost L. Induction of similar features of apoptosis in human and bovine vascular endothelial cells treated by 7-ketocholesterol. J Pathol 1997; 183:330–8.
[77] Pedruzzi E, Guichard C, Ollivier V, Driss F, Fay M, Prunet C, et al. NAD(P)H oxidase Nox-4 mediates 7-ketocholesterol-induced endoplasmic reticulum stress and apoptosis in human aortic smooth muscle cells. Mol Cell Biol 2004;24:10703–17.